Available online at www.sciencedirect.com
SCIENCE DIRECT
Biochemical Pharmacology 69 (2005) 1773–1784
Biochemical Pharmacology
www.elsevier.com/locate/biochempharm

# Involvement of Ras/extracellular signal-regulated kinase, but not Akt pathway in risedronate-induced apoptosis of U937 cells and its suppression by cytochalasin B

Hirofumi Fujita [a,b,*], Toshihiko Utsumi [c], Shikibu Muranaka [a], Tetsuya Ogino [d], Hiromi Yano [e], Jitsuo Akiyama [f], Tatsuji Yasuda [b], Kozo Utsumi [a]

[a] *Institute of Medical Science, Kurashiki Medical Center, Kurashiki 710-8522, Japan*
[b] *Department of Cell Chemistry, Institute of Molecular and Cell Biology, Okayama University Medical School, Okayama 700-8558, Japan*
[c] *Department of Biological Chemistry, Faculty of Agriculture, Yamaguchi University, Yamaguchi 753-8515, Japan*
[d] *Department of Pathological Research, Okayama University Graduate School of Medicine and Dentistry, Okayama 700-8558, Japan*
[e] *Department of Health and Sports Science, Kawasaki University of Medical Welfare, Kurashiki 701-0193, Japan*
[f] *Doonan Institute of Medical Science, Ishikawa-cho, Hakodate 041-8508, Japan*

Received 21 November 2004; accepted 9 March 2005

**Abstract**

Although risedronate, a nitrogen containing bisphosphonate (BPs), strongly inhibits bone resorption by enhanced apoptosis of osteoclasts, its mechanism remained unclear. In this study, we investigated the molecular mechanism of risedronate-induced apoptosis of U937 cells, with a focus on extracellular signal-regulated kinase 1/2 (ERK 1/2) and protein kinase B (Akt) pathways, mitochondria-mediated apoptosis, and the effect of disruption of the actin cytoskeleton. Risedronate facilitated the relocation of Ras from membrane to cytosol through inhibited isoprenylation. Accordingly, risedronate suppressed the phosphorylation of ERK 1/2, a downstream survival signaling kinase of Ras, affected the intracellular distribution of Bcl-xL, and induced the mitochondrial membrane depolarization, cytochrome c release, activated caspase cascade and DNA fragmentation. The risedronate-induced apoptosis was effectively suppressed with cyclosporine A plus trifluoperazine, potent inhibitors of mitochondrial membrane permeability transition (MPT). The risedronate-induced apoptosis was independent of Akt, another cAMP-dependent survival signaling kinase. Risedronate facilitated dephosphorylation of Bad at Ser112, an ERK phosphorylation site, but not at Ser136, an Akt phosphorylation site. All of these apoptosis-related changes induced by risedronate were strongly suppressed by cytochalasin B, an inhibitor of actin filament polymerization. These results indicate that risedronate-induced apoptosis in U937 cells involves Ras/ERK, but not Akt signaling pathway, and is dependent on MPT, and that disruption of the actin cytoskeleton inhibits the risedronate-induced apoptosis at its early step.


*Keywords:* Apoptosis; Bisphosphonate; Cytochalasin B; ERK1/2; Bad; Membrane permeability transition

## 1. Introduction

Bisphosphonates (BPs) are potent inhibitors of bone resorption and are used for the therapy of osteoporosis, Paget's disease, bone metastasis, and other bone diseases [1]. They are structurally similar to pyrophosphate and preferentially bind to hydroxyapatite of the bone. Bisphosphonates can be divided into two groups with distinct molecular mechanisms of action depending on the R2 side chain. One group is the BPs that lack nitrogen, such as clodronate and etidronate. This group does not inhibit protein prenylation and show weak inhibition of bone resorption activity [2,3]. The other group is nitrogen-containing BPs, such as alendronate, zoledronate and risedronate. This group strongly inhibits bone resorption and causes apoptosis of osteoclasts and other cell lines in vitro.

*Abbreviations:* ERK, extracellular signal-regulated kinase; PS, phosphatidylserine; BPs, bisphosphonates; AMC, 7-amino-4-methyl-coumarin; Ac-IETD-CHO, acetyl-Ile-Glu-Thr-Asp-CHO; JC-1, 5,5′,6,6′-tetrachloro-1,1′,3,3′-tetraethylbenzimidazol carbocyanine iodide; FPP, farnesyl pyrophosphate; GGOH, geranylgeraniol; s-GTP-bp, small GTP-binding proteins; MPT, membrane permeability transition; pCPT-cAMP, 8-(4-chlorophenylthio) adenosine 3′:5′-cyclic monophosphate

* Corresponding author. Tel.: +81 86 426 8616; fax: +81 86 426 8616.
*E-mail address:* fujita01@mx3.kct.ne.jp (H. Fujita).

0006-2952/$ – see front matter © 2005 Elsevier Inc. All rights reserved.
doi:10.1016/j.bcp.2005.03.006

The nitrogen containing BPs inhibit FPP synthase, thereby inhibiting the biosynthesis of farnesyl diphosphate and/or geranylgeranyl diphosphate [4–6]. These compounds are important membrane-anchoring molecules of small GTP-binding proteins (s-GTP-bp) such as Ras. Their shortage facilitates dissociation of Ras from the inner surface of the membrane, and decreases Ras-mediated growth signal, thereby inhibiting cell proliferation [7,8]. Indeed, zoledronate induced delocalization of p21ras (Ras) from the cell membrane in cancer cells [9,10], and the downstream kinase that mediates survival signal, namely ERK 1/2, has been reported to be suppressed [10,11]. In this context, geranylgeraniol (GGOH) which bypasses inhibition of FPP synthase and replenishes the cells with a substrate for protein geranylgeranylation blocked the BP-induced apoptosis of osteoclasts [2]. Moreover, the protein kinase B (Akt) pathway has also been suggested to be involved in zoledronate-induced apoptosis in human pancreatic cancer cells and endothelial cells [10,12], but not in other experimental model using HL-60 cells [11]. These results indicate that BP-induced apoptosis might depend on the cell type and the structure of R2 moiety in BPs.

Recent studies showed that mitochondria have an important role in the induction of apoptosis. It was reported that forced expression of the anti-apoptotic protein Bcl-2 attenuated BP-induced loss of cell viability and induction of DNA fragmentation in MDA-MB-231 cells and that zoledronate-mediated apoptosis was associated with a time and dose-related release of mitochondrial cytochrome c into the cytosol in two cell lines [13]. Furthermore, BP-induced mitochondrial membrane depolarization in osteoclasts and hematopoietic tumor cells was also reported [14,15]. However, it is not clear whether the BP-induced apoptosis depends on mitochondrial membrane permeability transition (MPT).

Nitrogen containing BPs cause disruption of the ruffled border and actin cytoskeleton of osteoclasts and induce apoptosis, because nitrogen containing BPs reduce geranylgeranylated proteins which regulate the cytoskeleton [16,17]. However, it is currently unknown whether actin cytoskeleton regulates nitrogen containing BPs-induced apoptosis. In this context, cytochalasins, inhibitor of actin filament polymerization, has an ability to stimulate or suppress cell apoptosis through different mechanisms [18–22]. Thus, it is interesting to study how cytochalasin B affect on BP-induced apoptosis of U937 cells.

In this study, therefore, molecular mechanism of risedronate-induced apoptosis on U937 cells and its sensitivity to cytochalasin B were investigated. Our results indicated that the risedronate-induced apoptosis involved Ras/ERK, but not Akt pathway, and depended on mitochondrial MPT. We also found that cytochalasin B strongly suppressed the apoptosis-related changes in U937 cells by risedronate.

## 2. Materials and methods

### 2.1. Chemicals

Cyclosporine A, 8-(4-chlorophenylthio) adenosine 3′:5′-cyclic monophosphate (pCPT-cAMP), cytochalasin B, demecolcine, farnesol and GGOH were obtained from Sigma. TACS$^{TM}$ Annexin V-FITC kit is obtained from Trevigen. 5,5′6,6′-Tetrachloro-1,1′,3,3′-tetraethyl- benzimidazolylcarbo-cyanine iodide (JC-1) was from Molecular Probes. Polyclonal antibody of Bid was from Genzyme-Techne. Monoclonal antibody of actin was from CHEMICON. Bcl-2 (N-19), Bax (Δ21) and Bcl-xL (S-18) polyclonal antibodies were from Santa Cruz Biotechnology. Polyclonal antibodies against Akt, ERK, Bad, phospho-Akt (p-Akt) (Ser473), phospho-ERK1/2 (p-ERK) (Thr202/Tyr204), phospho-Elk-1 (p-Elk-1) (Ser383), phospho-GSK-3β (p-GSK-3β) (Ser9), phospho-FKHR (p-FKHR) (Ser256), phospho-Bad (p-Bad) (Ser112) and p-Bad (Ser136) were from Cell Signaling Technology. Polyclonal antibody of Bad for intracellular localization was from BD Transduction Laboratories. Polyclonal antibody of cytochrome c was from Pharmingen. Monoclonal antibody of Ras was from CALBIOCHEM. Can Get Signal$^{TM}$ was from TOYOBO. Fluorogenic tetrapeptide substrates, such as Ac-DEVD-MCA (for caspase-3), Ac-IETD-MCA (for caspase-8) and Ac-LEHD-MCA (for caspase-9), and Ac-IETD-CHO (for caspase-8 inhibitor) were from the Peptide Institute. Risedronate was donated from Ajinomoto.

### 2.2. Cell line

U937 was obtained from RIKEN Cell Bank and was maintained in RPMI 1640 supplemented with 10% heat-inactivated fetal bovine serum, 100 U/ml penicillin and 100 μg/ml streptomycin. Cells were grown in a humidified incubator at 37 °C under 5% $CO_2$/95% air. Cells were plated onto 35 mm and 100 mm dishes ($0.2 \times 10^5$ cells/ml) in 2 ml and 20 ml of RPMI 1640 containing 10% fetal bovine serum, respectively, and incubated for 16 h before treatment with various reagents.

### 2.3. Analysis for PS exposure

PS exposed on the outside of the cells was determined by TACS$^{TM}$ Annexin V-FITC kit. Briefly, cells were washed with cold PBS, pelleted and resuspended in 100 μl annexin V-FITC diluted 3:100 in binding buffer (10 mM Hepes, 100 mM NaCl, 10 mM KCl, 1 mM $MgCl_2$, 1.8 mM $CaCl_2$) containing propidium iodide (1:10). Cells were incubated for 15 min at room temperature, then the stained cells were observed by fluorescence microscopy. Total cells (1000–1500 cells) and FITC positive cells were counted in the same field, and annexin V positive rate (%) was calculated.

### 2.4. Analysis for DNA fragmentation

The extent of DNA fragmentation was determined spectrophotometrically by the diphenylamine method as described in the previous papers [23,24]. DNA ladder formation was also observed by agarose gel electrophoresis as described in the previous paper [25].

### 2.5. Subcellular fractionation

After harvesting cells, $1 \times 10^7$ cells were suspended in 50 μl of ice-cold buffer A [250 mM sucrose, 20 mM HEPES buffer (pH 7.5), 10 mM KCl, 1.5 mM $MgCl_2$, 1 mM EGTA, 1 mM dithiothreitol and 0.1 mM PMSF] and homogenized in a Teflon Potter-Elvehjem homogenizer. The homogenate was centrifuged at $750 \times g$ for 10 min at 4 °C. The supernatant was then centrifuged at $16{,}000 \times g$ for 10 min at 4 °C. The resulting pellet (mitochondrial fraction) was resuspended in buffer A to conform to the volume of cytosolic fraction. The supernatant was further centrifuged at $100{,}000 \times g$ for 60 min at 4 °C. The final supernatant represented the cytosolic fraction (cytosol). Aliquots were used for Western blot analysis of cytochrome c, Bcl-2, Bcl-xL, Bad and Bax.

Analysis of Ras distribution in the cells was carried out as described in previous paper [26]. Cells were resuspended in 40 mM Tris–HCl (pH 7.5) containing 10 mM $MgCl_2$, 2 mM $CaCl_2$, 250 mM sucrose, and 1 mM PMSF, and lysed by three cycles of freezing at −80 °C and thawing. The lysate was separated into supernatant (cytosol) and precipitate (membrane) fractions by centrifugation at $200{,}000 \times g$ for 35 min at 4 °C. Aliquots of 50 μg protein were used for Western blot analysis of Ras.

### 2.6. Cell lysates for Western blot analysis

After U937 cells ($1 - 2 \times 10^6$) were harvested, they were suspended for 30 min in ice-cold lysis buffer [20 mM Tris–HCl (pH 7.5), 150 mM NaCl, 1% Triton X-100, 1 mM EDTA, 1 mM EGTA, with the addition of 1 mM $Na_3VO_4$ and 20 mM sodium β-glycerophosphate for analysis of Akt, p-Akt, ERK, p-ERK, p-Elk-1 (Ser383), p-GSK-3β (Ser9), p-FKHR (Ser256), Bad, p-Bad (Ser112) and p-Bad (Ser136)] supplemented with protease inhibitors (0.1 mM PMSF, 2 μg/ml aprotinin, 100 μg/ml leupeptin and 5 μg/ml pepstatin A). Lysates were cleared by centrifugation at $20{,}000 \times g$ for 10 min at 4 °C. The aliquots of 50 μg supernatant proteins were used for Western blot analysis of Bid, Akt, p-Akt, ERK, p-ERK, p-Elk-1 (Ser383), p-GSK-3β (Ser9), p-FKHR (Ser256), Bad, p-Bad (Ser112), p-Bad (Ser136) and actin as described in previous paper [27]. During immunoreaction of p-Bad (Ser112) and p-Bad(Ser136), we used Can Get Signal™. Protein concentration was determined by the method of Bradford [28] using bovine serum albumin as a standard.

### 2.7. Assay for caspase activity

Activity of caspase was determined as described previously [24] in 20 mM HEPES buffer (pH 7.5) containing

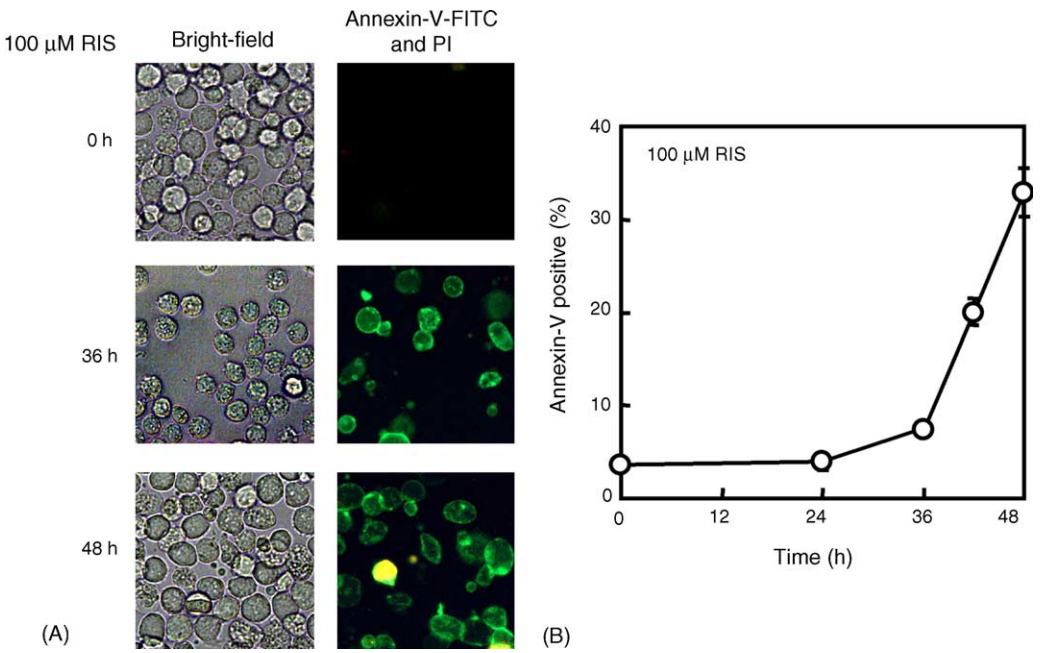


Fig. 1. Risedronate-induced phosphatidylserine exposure in U937 cells. (A) U937cells were treated for the indicated times with 100 μM risedronate, stained with annexin V-FITC and propidium iodide and observed by light and fluorescence microscopy. (B) In (A), total cells (1000–1500 cells) and FITC positive cells were counted in the same field, and percentage of annexin V positive rate was calculated. Data showed means ± S.D. from triplicate experiments. PS, RIS and PI are phosphatidylserine, risedronate and propidium iodide, respectively.

0.1 M NaCl and 5 mM DTT 37 °C using 10 μM of acetyl-Asp-Glu-Val-Asp-MCA, acetyl-Leu-Glu-His-Asp-MCA and acetyl-Ile-Glu-Thr-Asp-MCA for caspase-3, -9 and -8, respectively. One unit of the enzyme was defined as the amount of enzyme required for the liberation of 1 nmol of AMC during 1 h. Fluorescence of released AMC was measured using a fluorospectrophotometer with the excitation and emission wavelengths of 355 and 460 nm, respectively.

### 2.8. Assay of intracellular mitochondrial membrane potential

After incubation with risedronate for 48 h, cells were washed twice with phosphate buffer saline (PBS) and stained with 5 μg/ml of JC-1 for 30 min at 37 °C. Then, cells were analyzed using a FACS Calibur flow cytometer (Becton Dickinson) to determine the mitochondrial membrane potential [29].

### 2.9. Statistical analysis

Results are expressed as the mean ± S.D. The significance of differences between experimental conditions was determined using the two-tailed Student's *t*-test. A probability of $p < 0.05$ was considered significant.

## 3. Results

### 3.1. Risedronate-induced apoptosis and its sensitivity to MPT inhibitors and prenyl compounds

Risedronate induced PS exposure in a time dependent manner (Fig. 1) and DNA fragmentation in a concentration and time dependent manner (Fig. 2A and B). These apoptotic events were detected clearly at 36 h and increased steadily for up to 48 h after the treatment with 100 μM risedronate. At this time, DNA ladder was detected on 2%

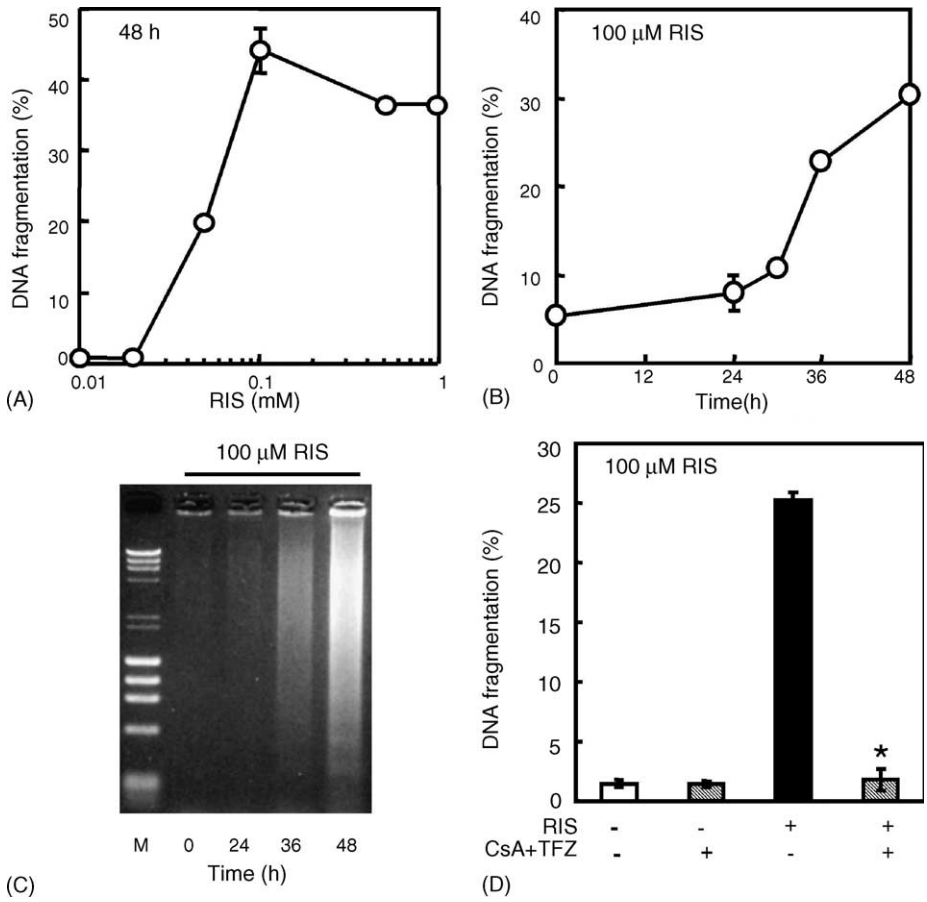


Fig. 2. Risedronate-induced DNA fragmentation in U937 cells and its sensitivity to MPT inhibitors. (A) U937 cells were treated with various concentrations of risedronate for 48 h. DNA fragmentation was assessed by the diphenylamine method. (B) U937 cells were treated for the indicated times with 100 μM risedronate. (C) Electrophoretic patterns of DNA from the cells ($2 \times 10^5$) treated for 24, 36 and 48 h with 100 μM risedronate. (D) Sensitivity of risedronate-induced DNA fragmentation to cyclosporine A plus trifluoperazine, inhibitors of MPT. U937 cells were preincubated with 0.5 μM cyclosporine A plus 5 μM trifluoperazine for 2 h and then incubated for 48 h with 100 μM risedronate. Data showed means ± S.D. from triplicate experiments. The asterisk indicated that cyclosporine A plus trifluoperazine significantly inhibited risedronate-induced DNA fragmentation ($p < 0.05$). RIS, CsA and TFZ are risedronate, cyclosporine A and trifluoperazine, respectively.

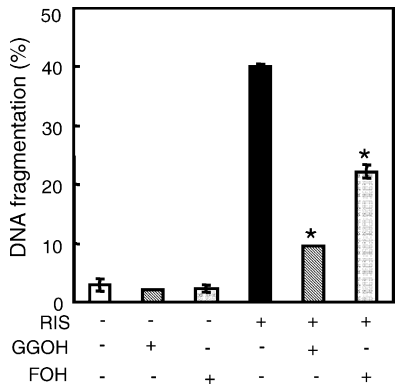


Fig. 3. Effects of geranylgeraniol and farnesol on risedronate-induced DNA fragmentation. Experimental conditions were the same as described in Fig. 2. U937 cells were preincubated with 10 μM geranylgeraniol or 20 μM farnesol for 2 h and then incubated for 48 h with 100 μM risedronate. Data showed means ± S.D. from triplicate experiments. The asterisk indicated that geranylgeraniol and farnesol significantly inhibited risedronate-induced DNA fragmentation ($p < 0.05$). GGOH and FOH are geranylgeraniol and farnesol, respectively.

agarose gel electrophoresis (Fig. 2C). The DNA fragmentation was almost completely suppressed by the pretreatment with mitochondrial MPT inhibitors, namely cyclosporine A plus trifluoperazine (Fig. 2D). In addition, pretreatment with GGOH and farnesol suppressed the DNA fragmentation in U937 cells (Fig. 3).

### 3.2. Inhibition of the DNA fragmentation by cytochalasin B, but not by demecolcine

Cytochalasin B, which inhibits actin filament polymerization, suppressed the risedronate-induced DNA fragmentation as well as nuclear fragmentation in a concentration dependent manner (Fig. 4A–C). However, demecolcin, which inhibits microtubules polymerization, did not suppress the DNA fragmentation (Fig. 4A).

### 3.3. Activation of caspases and their sensitivity to cytochalasin B and MPT inhibitors

The activities of various caspases were examined using specific synthetic substrates for the enzymes. Risedronate activated caspase-3 like activity in a concentration dependent manner in U937 (Fig. 5A). The activation of caspase-3 like activity occurred at similar risedronate concentration to that of DNA fragmentation (Figs. 2A and 5A). Risedronate also activated caspase-9 and -8 like activities (Fig. 5C and D), although their activities were substantially

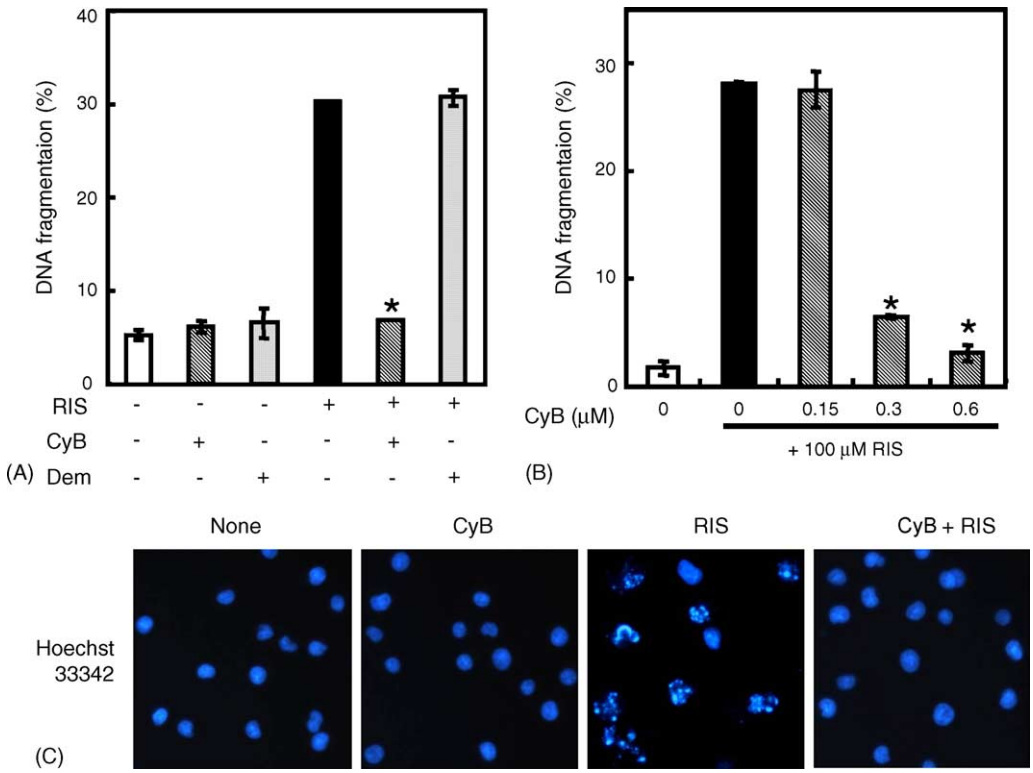


Fig. 4. Effect of cytochalasin B and demecolcine on risedronate-induced DNA fragmentation. Experimental conditions were the same as described in Fig. 2A. (A) Cells were preincubated with 0.6 μM cytochalasin B or 1 ng/ml demecolcine for 2 h and then treated with 100 μM risedronate for 48 h. (B) Concentration-dependent suppression of risedronate-induced DNA fragmentation by cytochalasin B. Cells were preincubated with indicated concentrations of cytochalasin B for 2 h and then incubated for 48 h with 100 μM risedronate. (C) Inhibition of risedronate-induced nuclear fragmentation by cytochalasin B. Cells were preincubated with 0.6 μM cytochalasin B for 2 h and then treated with 100 μM risedronate for 48 h, and then stained with Hoechst33342 and observed with fluorescence microscopy. Similar results were obtained in three separate experiments. Data showed means ± S.D. from triplicate experiments. The asterisk indicated that cytochalasin B significantly inhibited risedronate-induced DNA fragmentation ($p < 0.05$). CyB and Dem are cytochalasin B and demecolcine, respectively.

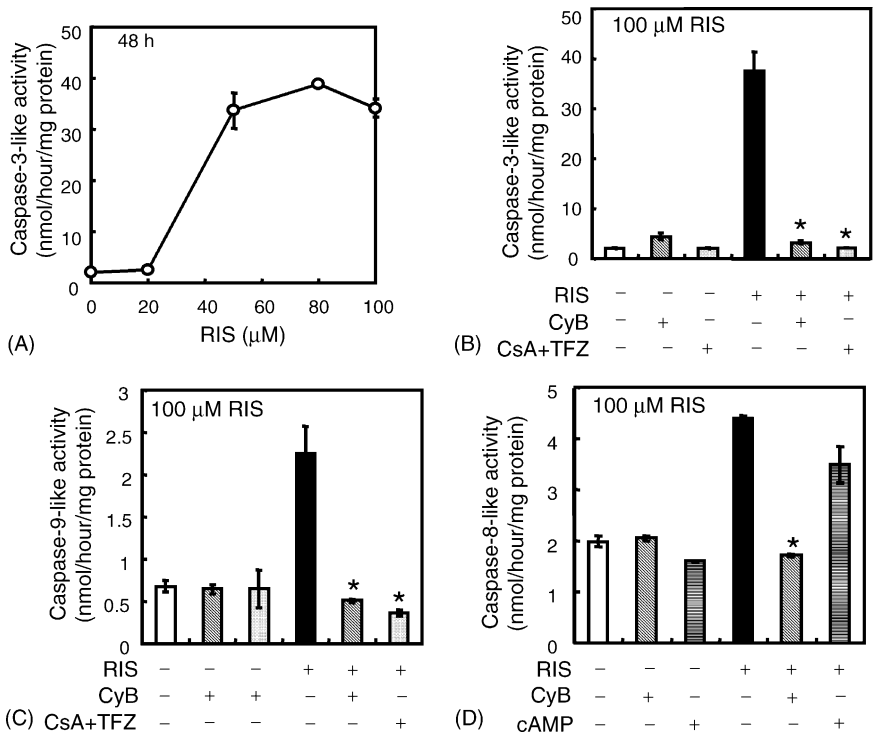


Fig. 5. Activation of caspases by risedronate and their sensitivity to cytochalasin B, cyclosporine A plus trifluoperazine and cAMP. The activities of various caspases were measured by using synthetic peptide substrates (Ac-DEVD-MCA for caspase-3, Ac-IETD-MCA for caspase-8 and Ac-LEHD-MCA for caspase-9) after treatment with risedronate. (A) Dose-dependency of risedronate-induced caspase-3 like protease activity. Cells were incubated with various concentrations of risedronate for 48 h. (B–D) U937 cells were preincubated with the indicated reagents for 2 h and then incubated with 100 μM risedronate for 48 h. (B, C) Effects of cytochalasin B, and cyclosporine A plus trifluoperazine on the risedronate-induced caspase-3 like (B) and caspase-9 like (C) protease activation. Used concentrations of cytochalasin B, cyclosporine A plus trifluoperazine were 0.6 μM, 0.5 μM and 5 μM, respectively. (D) Effects of cytochalasin B and pCPT-cAMP on the risedronate-induced activation of caspase-8 like activity. The used concentrations of cytochalasin B and pCPT-cAMP were 0.6 μM and 100 μM, respectively. Data showed means ± S.D. from triplicate experiments. The asterisk indicated that cyclosporine A and cytochalasin B significantly inhibited risedronate-induced caspase activations ($p < 0.05$). RIS, CyB, CsA, TFZ and cAMP are risedronate, cytochalasin B, cyclosporine A, trifluoperazine and pCPT-cAMP, respectively.

lower than that of caspase-3 like enzyme. Cytochalasin B almost completely suppressed the activation of the three caspases (Fig. 5B–D). Mitochondrial MPT inhibitors also strongly suppressed caspase-3 and -9 activation (Fig. 5B and C).

### 3.4. Functions of mitochondria and their sensitivity to cytochalasin B and MPT inhibitors

Since risedronate activated caspase-9, which is typically activated following cytochrome c release from mitochondria, we investigated whether risedronate induce cytochrome c release in U937 cells. Significant fraction of cytochrome c was released from mitochondria into cytosol after risedronate treatment, and the release was suppressed by 0.6 μM cytochalasin B and 10 μM GGOH (Fig. 6).

Since the cytochrome c release by pore opening of MPT is characterized by mitochondrial membrane depolarization [30], we studied the effect of risedronate on membrane potential of mitochondria and its sensitivity to cytochalasin B and MPT inhibitors. Risedronate induced the depolarization at 48 h after incubation with risedronate in a concentration-dependent manner (Fig. 7C). The depolarization was potently suppressed by preincubation with cytochalasin B or MPT inhibitors (Fig. 7A and B).

### 3.5. Role of Akt/caspase-8/Bid cleavage pathway in the DNA fragmentation

Since risedronate induced the activation of caspase-8, which can works before cytochrome c release and caspase-3 activation, we studied the effect of Ac-IETD-CHO, a specific inhibitor of caspase-8, on the caspase-3 activity in U937 cells. No distinguishable effect of Ac-IETD-CHO on the caspase-3 activity was observed at 48 h after the treatment with 100 μM risedronate (Fig. 8A).

Caspase-8 can cleave Bid, and then the truncated Bid can mediate cytochrome c release from mitochondria [31–33]. Western blot analysis revealed that Bid was present as a 22 kDa protein in U937 cells. However, truncated Bid was not observed at 48 h after treatment with 100 μM risedronate (Fig. 8B).

We reported previously that p-Akt has an important role in the activation of caspase-8 and cleavage of Bid [34], and that the cellular level of p-Akt is regulated by cAMP through a phosphoinositide (PI) 3-kinase dependent path-

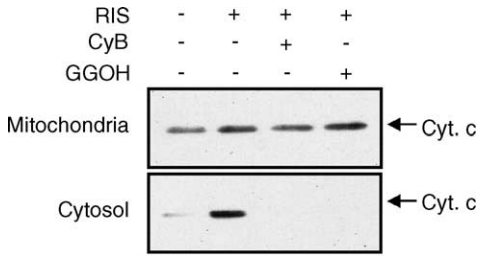


Fig. 6. Risedronate-induced cytochrome c release and its sensitivity to cytochalasin B and geranylgeraniol. U937 cells were preincubated with cytochalasin B or geranylgeraniol for 2 h and then incubated with 100 μM risedronate for 48 h. Cytochrome c in mitochondrial and cytosolic fractions was detected by western blotting using anti-cytochrome c antibody. Lane1; none treated, lane 2; risedronate, lane 3; risedronate plus 0.6 μM cytochalasin B, lane 4; risedronate plus 10 μM geranylgeraniol. Similar results were obtained in three separate experiments. CyB and GGOH are cytochalasin B and geranylgeraniol, respectively.

way [35,36]. Thus, we examined the effect of pCPT-cAMP, a membrane-permeable cAMP, on the risedronate-induced activation of caspase-8. As a result, the pCPT-cAMP did not affect the risedronate-induced activation of caspase-8 (Fig. 5D). Moreover, we examined the effect of risedronate on the cellular levels of Akt and p-Akt as well as the phosphorylation status of Akt downstream substrates including GSK-3β (Ser9), FKHR (Ser256) and Bad (Ser136). The levels of Akt and p-Akt proteins did not decrease by 100 μM risedronate (Fig. 8C). The phosphorylation status of Akt substrates did not change either. In addition, pCPT-cAMP and cytochalasin B had no effects on Akt protein levels and its phosphorylation status.

### 3.6. Risedronate-induced downregulation of Ras/ERK signaling pathway and its sensitivity to cytochalasin B and GGOH

Since risedronate inhibits FPP synthase, the intracellular distribution of Ras was examined, which normally localizes on the inner surface of the cell membrane through farnesyl anchor. After the treatment with risedronate, the level of Ras in cytoplasm was increased with a decrease in membrane fraction, and the distribution was restored by the preincubation with cytochalasin B and GGOH (Fig. 9).

The protein levels and the phosphorylation status of ERK 1/2, which is a downstream signaling molecule of the prenylated s-GTP-bp such as Ras [9,11], were studied. Risedronate suppressed the phosphorylation of ERK in a

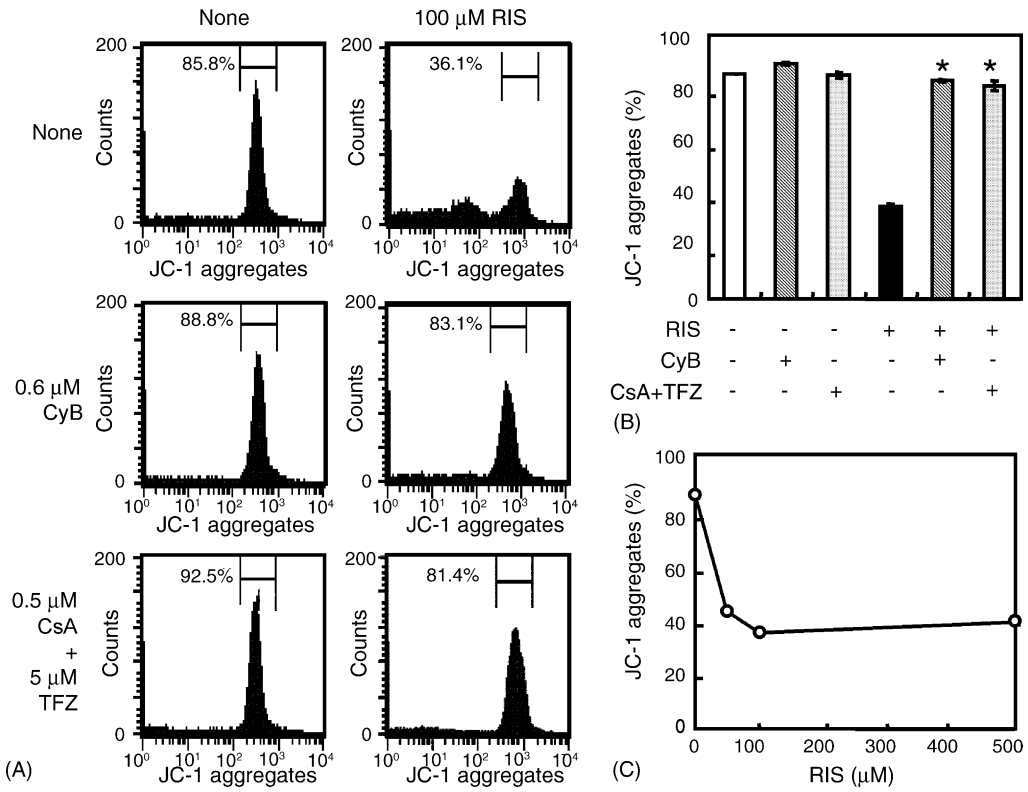


Fig. 7. Risedronate-induced mitochondrial depolarization of U937 cells and its sensitivity to cytochalasin B and cyclosporine A plus trifluoperazine. Mitochondrial membrane potential was detected by fluorescence of JC-1 and quantified by using a FACScan flow cytometer. (A) Cells were preincubated with or without 0.6 μM cytochalasin B or 0.5 μM cyclosporine A plus 5 μM trifluoperazine for 2 h and then incubated with 100 μM risedronate for 48 h. (B) Quantitative analysis of the data depicted in panel A is shown. (C) Dose-dependency of risedronate-induced depolarization. Cells were incubated with indicated concentrations of risedronate for 48 h. Similar results were obtained in three separate experiments. The asterisk indicated that cytochalasin B and cyclosporine A plus trifluoperazine significantly inhibited risedronate-induced mitochondrial depolarization ($p < 0.05$). RIS, CyB, CsA and TFZ are risedronate, cytochalasin B, cyclosporine A and trifluoperazine, respectively.

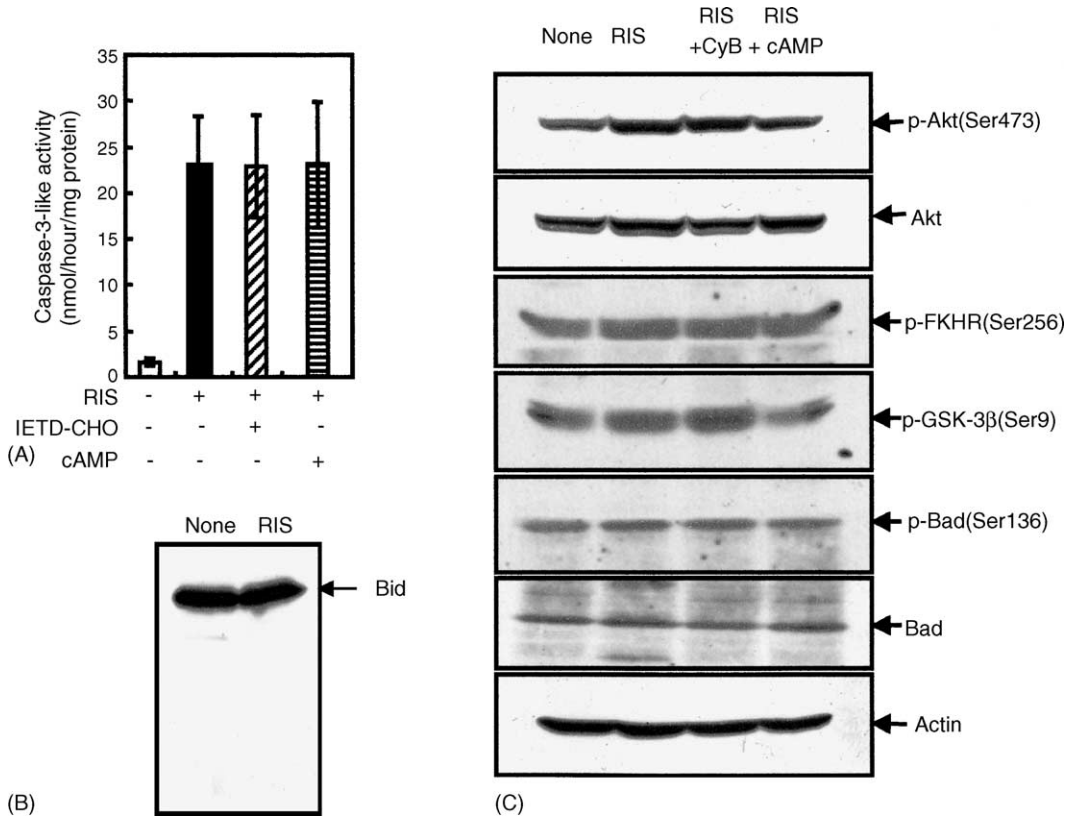


Fig. 8. Effect of risedronate on the Akt/caspase-8/Bid cleavage pathway. Experimental conditions were the same as described in Fig. 6. (A) Effect of pCPT-cAMP and caspase-8 inhibitor, Ac-IETD-CHO, on caspase-3 like activity. Cells were preincubated for 2 h in the presence or absence of 100 μM cAMP and 100 μM Ac-IETD-CHO and then cells were incubated with 100 μM risedronate for 48 h. Caspase-3 like activity was determined as in Fig. 5. Data show means ± S.D. from triplicate experiments. (B) Effect of risedronate on the cleavage of Bid. Bid was detected by Western blotting with anti-Bid antibody. Cells were treated with or without 100 μM risedronate for 48 h. Similar results were obtained in three separate experiments. (C) Effect of risedronate on Akt and its downsteam substrates and their sensitivity to cytochalasin B and pCPT-cAMP. Cells were pretreated with 0.6 μM cytochalasin B or 100 μM pCPT-cAMP for 2 h and subsequently with or without 100 μM risedronate for 30 h. p-Akt (Ser473), Akt, p-FKHR (Ser256), p-GSK-3β (Ser9), p-Bad (Ser136) and Bad were detected by Western blotting with each specific antibody. As a control for protein loading, Western blot analysis of actin was also carried out. Similar results were obtained in three separate experiments. IETD and cAMP are Ac-IETD-CHO and pCPT-cAMP, respectively.

time dependent manner (Fig. 10A). The risedronate-induced suppression of p-ERK occurred prior to PS exposure and DNA fragmentation (Figs. 1B and 2B). Consistent with this suppression of ERK phosphorylation, the phosphorylation of ERK downstream substrates, namely Elk-1 (Ser383) and Bad (Ser112), was also decreased by risedronate. The suppressed phosphorylation of ERK and its downstream substrates were restored by the preincubation of cytochalasin B and GGOH (Fig. 10B).

### *3.7. Effect of risedronate on the level and distributions of Bcl-2 family proteins and their sensitivity to cytochalasin B and GGOH*

Protein kinases such as Akt and ERK have been reported to promote cell survival through the regulation of some Bcl-2 family proteins [37,38]. In addition, risedronate-induced apoptosis was dependent on mitochondrial MPT which is generally regulated by Bcl-2 family proteins [37]. Therefore, the effect of risedronate on the level and distribution of Bcl-2 family proteins were examined. No changes in the level and distribution of Bax, Bcl-2 and Bad were observed by the treatment with risedronate. By contrast, Bcl-xL protein decreased substantially from the cytosolic fraction after the treatment with risedronate, whereas the Bcl-xL in mitochondrial fraction did not decrease. This reduction was rescued by the presence of cytochalasin B and GGOH (Fig. 11).

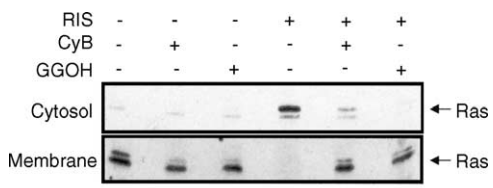


Fig. 9. Effect of risedronate on the distribution of Ras in cells and its sensitivity to cytochalasin B and geranylgeraniol. Experimental conditions were the same as described in Fig. 8. Cells were pretreated with 0.6 μM cytochalasin B or 100 μM geranylgeraniol for 2 h and subsequently with 100 μM risedronate for 15 h. Ras in membrane and cytosolic fractions was detected by Western blotting with anti-Ras antibody. Similar results were obtained in three separate experiments.

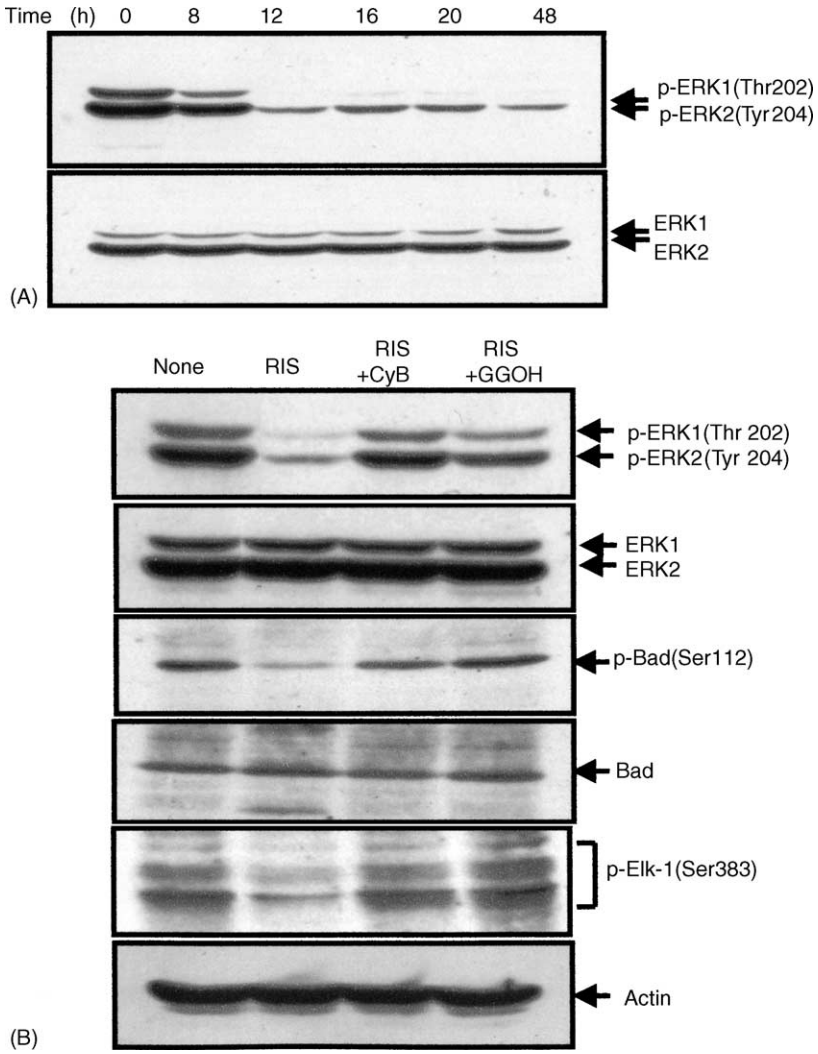


Fig. 10. Effect of risedronate on the levels of ERK 1/2 and p-ERK 1/2 in risedronate-treated U937 cells and their sensitivity to cytochalasin B and geranylgeraniol. Experimental conditions were the same as described in Fig. 8. (A) Time-dependent changes of p-ERK. Cells were treated for the indicated times with 100 μM risedronate and ERK 1/2 and p-ERK 1/2 (Thr202/Tyr204) were detected by Western blotting with each specific antibody. (B) Effect of cytochalasin B and geranylgeraniol on ERK 1/2 and its downstream substrates in the risedronate-treated cells. Cells were pretreated with 0.6 μM cytochalasin B or 10 μM geranylgeraniol for 2 h and subsequently with or without 100 μM risedronate for 48 h. p-ERK(Thr202/Tyr204), ERK, p-Bad (Ser112), Bad and p-Elk-1 (Ser383) were detected by Western blotting with each specific antibody. As a control for protein loading, Western blot analysis of actin was also carried out. Similar results were obtained in three separate experiments.

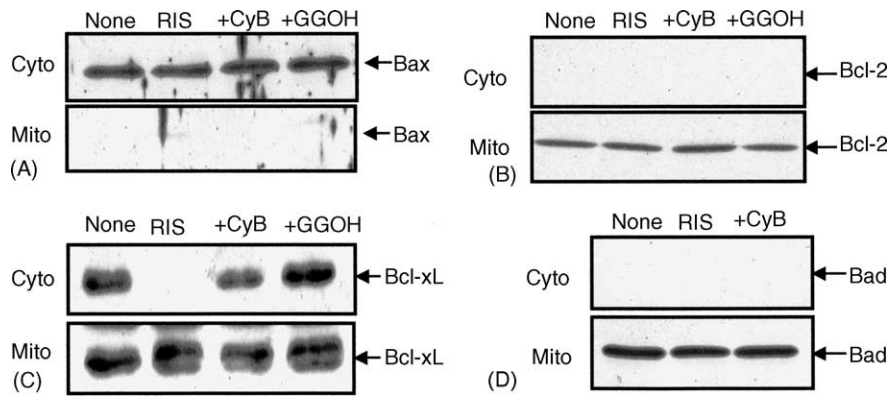


Fig. 11. Changes in the distribution of Bcl-2 family proteins in risedronate-treated U937 cells and their sensitivity to cytochalasin B and geranylgeraniol. Experimental conditions were the same as described in Fig. 6. Cells were pretreated with 0.6 μM cytochalasin B or 10 μM geranylgeraniol for 2 h and subsequently with or without 100 μM risedronate for 48 h. Bax (A), Bcl-2 (B), Bcl-xL (C) and Bad (D) in mitochondrial and cytosolic fractions were detected by Western blotting with each antibody. Similar results were obtained in three independent experiments.

## 4. Discussion

In the present study, we showed the molecular mechanism of risedronate-induced apoptosis of monocyte-like U937 cells. Our results suggested the apoptosis of U937 cells was induced by mitochondrial MPT through Ras/ERK but not Akt pathway. All of the apoptosis-related changes induced by risedronate were strongly suppressed by cytochalasin B. Cytochalasin B seemed to inhibit the apoptosis at its early step.

3-Hydroxy-3-methylglutaryl-CoA reductase enhances sterol and isoprenoid synthesis, and increases the prenylation of s-GTP-bps [39]. Previously, we observed that mevastatin, an inhibitor of HMG-CoA-R, induced apoptosis of HL-60 cells through a GGOH inhibitable mechanism [40]. Nitrogen containing BPs inhibit the FPP synthesis and the membrane localization of s-GTP-bp through suppressed prenylation with farnesyl or geranylgeranyl isoprenoid group, and thus suppressed post-translational modification of s-GTP-bps [7,10]. In fact, it has been reported that zoledronate impaired Ras membrane localization and induced cytochrome c release in breast cancer cells [41]. Thus, BPs might inhibit the signal transduction from prenylated s-GTP-bp to ERK [42]. In the present experiment, we observed that risedronate stimulated translocation of Ras in cytosol from cell membranes and suppressed the phosphorylation of ERK and its downstream substrates in a GGOH inhibitable mechanism (Figs. 9 and 10). These results suggested that risedronate-induced apoptosis of U937 cells occurred through Ras/ERK 1/2 pathway.

In the present experiment, we observed that ERK was markedly dephosphorylated at 12 h after risedronate treatment, but apoptosis, which was detected by PS exposure and DNA fragmentation, was not obvious until 36 hours (Figs. 1, 2B and 10A). These results revealed the existence of time lag between dephosphorylation of ERK and apoptosis. This time lag may indicate that the series of events from ERK dephosphorylation to apoptosis require substantial time, or that the decrease in ERK signal is not sufficient for apoptosis and additional apoptosis-inducing signal is required.

Accumulated evidences indicate that ERK might regulate the apoptosis through expression or phosphorylation of Bcl-2 family proteins [37,38]. It has been reported that constitutively active MEK, Ras, or Raf-1, like B-Raf, prevented apoptosis after growth factor deprivation, and that the B-Raf (Ras)/MEK/ERK pathway conferred protection against apoptosis at the level of caspase activation, downstream of cytochrome c release [42,43]. Ras/Raf/MEK/ERK pathway is involved in maintaining cell survival by modulating the activity of apoptosis regulating molecules including Bad [44]. Non-phosphorylated Bad can promote apoptosis by binding to Bcl-xL and abrogating its function that suppresses mitochondrial MPT [37]. Serine112 and 136 of Bad is phosphorylated by ERK pathway and Akt pathway, respectively, and this phosphorylation decreases Bad-Bcl-xL binding affinity [44,45]. In the present experiment, we observed that Akt pathway signaling and serine136 phosphorylation of Bad was not decreased by risedronate treatment, whereas ERK pathway signaling and phosphorylation at serine112 of Bad was decreased (Figs. 8C and 10B). These findings suggested that dephosphorylation of Bad by the decrease in kinase activity of ERK, but not Akt, might promote apoptosis through the mitochondrial apoptosis pathway. Actually, in the present experiment, we observed that the level of cytosolic Bcl-xL decreased significantly, whereas mitochondrial localization of Bad was not affected by risedronate treatment (Fig. 11). As the dephosphorylation of Bad enhances Bad-Bcl-xL binding, these findings suggested that cytosolic Bcl-xL might be translocated to mitochondria to bind Bad. Moreover, our results also indicated that the risedronate-induced apoptosis depended on mitochondrial MPT. In fact, risedronate induced depolarization and cytochrome c release (Figs. 6 and 7), and the risedronate-induced apoptosis was strongly inhibited by cyclosporine A plus trifluoperazine, blockers of the mitochondrial MPT (Figs. 2, 6 and 7) [46]. Thus, it is likely that risedronate-induced apoptosis was due to the enhancement of mitochondrial MPT through the impaired function of Bcl-xL, which resulted from Bad-Bcl-xL binding.

Another proposed mechanism of apoptosis by BP is the inhibition of protein kinase B (Akt) pathway [10,12]. In the present experiment, however, we found that risedronate did not affect Bid cleavage, the phosphorylation of Akt and its downstream substrates in U937 cells. Furthermore, cAMP and an inhibitor of caspase-8, Ac-IETD-CHO, did not affect the caspase-3 activity (Fig. 8). These results indicated that Ras/Akt pathway was not involved in risedronate-induced apoptosis of U937 cells and that risedronate-induced activation of caspase-8 might be the results of caspase-3 activation [47].

In relation to the involvement of actin cytoskeletal architecture in BP-induced apoptosis, it is plausible that cytochalasin B inhibited the uptake of risedronate into the cell. It has been reported that cytochalasins can inhibit apoptosis in articular chondrocytes, B lymphoma cells and lymphocytes [20–22]. Furthermore, cytochalasins can also inhibit endocytosis [48–50] and translocation of BP into the cell occurred through endocytosis [51,52]. In addition, our experiments showed that cytochalasin B restored all the risedornate-induced changes. Thus, cytochalasin B appeared to inhibit the effects of risedronate somewhere at the earlier step, including its uptake into the cell. To elucidate the anti-apoptotic mechanism of cytochalasins is our next subject.

From these results, it was concluded that Ras/ERK has an important role in the mechanism of risedronate-induced apoptosis of U937 cells and that the apoptosis mechanism and bone resorption inhibition of osteoclasts by risedronate might be mediated by actin cytoskeleton at upstream of FPP synthase inhibition.

## Acknowledgements

This work was supported, in part, by grants from the Ministry of Education, Science and Culture of Japan, the Eisai Co. and the Japan Keirin Association. We would also like to thank to Ajinomoto Co. Ltd for the kindly donating the risedronate for these experiments.

## References

[1] Rodan GA. Mechanisms of action of bisphosphoneates. Annu Rev Pharmacol Toxicol 1998;38:375–88.
[2] Reszka AA, Halasy-Nagy JM, Masarachia PJ, Rodan GA. Bisphosphonates act directly on the osteoclast to induce caspase cleavage of Mst1 kinase during apoptosis. A link between inhibition of the mevalonate pathway and regulation of an apoptosis-promoting kinase. J Biol Chem 1999;274:34967–73.
[3] Lehenkari PP, Kellinsalmi M, Napankangas JP, Ylitalo KV, Monkkonen J, Rogers MJ, et al. Further insight into mechanism of action of clodronate: inhibition of mitochondrial ADP/ATP translocase by a nonhydrolyzable, adenine-containing metabolite. Mol Pharmacol 2002;61:1255–62.
[4] Hughes DE, Wright KR, Uy HL, Sasaki A, Yoneda T, Roodman GD, et al. Bisphosphonates promote apoptosis in murine osteoclasts in vitro and in vivo. J Bone Miner Res 1995;10:1478–87.
[5] Luckman SP, Hughes DE, Coxon FP, Graham R, Russell G, Rogers MJ. Nitrogen-containing bisphosphonates inhibit the mevalonate pathway and prevent posttranslational prenylation of GTP-binding proteins, including Ras. J Bone Miner Res 1998;13:581–9.
[6] Fisher JE, Rogers MJ, Halasy JM, Luckman SP, Hughes DE, Masarachia PJ, et al. Alendronate mechanism of action: geranylgeraniol, an intermediate in the mevalonate pathway, prevents inhibition of osteoclast formation, bone resorption, and kinase activation in vitro. Proc Natl Acad Sci USA 1999;96:133–8.
[7] Shipman CM, Rogers MJ, Apperley JF, Russell RG, Croucher PI. Bisphosphonates induce apoptosis in human myeloma cell lines: a novel anti-tumour activity. Br J Haematol 1997;98:665–72.
[8] Lee MV, Fong EM, Singer FR, Guenette RS. Bisphosphonate treatment inhibits the growth of prostate cancer cells. Cancer Res 2001;61:2602–8.
[9] Senaratne SG, Pirianov G, Mansi JL, Arnett TR, Colston KW. Bisphosphonates induce apoptosis in human breast cancer cell lines. Br J Cancer 2000;82:1459–68.
[10] Tassone P, Tagliaferri P, Viscomi C, Palmieri C, Caraglia M, D'Alessandro A, et al. Zoledronic acid induces antiproliferative and apoptotic effects in human pancreatic cancer cells in vitro. Br J Cancer 2003;88:1971–8.
[11] Nishida S, Fujii Y, Yoshioka S, Kikuichi S, Tsubaki M, Irimajiri K. A new bisphosphonate, YM529 induces apoptosis in HL-60 cells by decreasing phosphorylation of single survival signal ERK. Life Sci 2003;73:2655–64.
[12] Bezzi M, Hasmim M, Bieler G, Dormond O, Ruegg C. Zoledronate sensitises endothelial cells to tumor necrosis factor-induced programmed cell death: evidence for the suppression of sustained activation of focal adhesion kinase and protein kinase B/Akt. J Biol Chem 2003;278:43603–14.
[13] Senaratne SG, Mansi JL, Colston KW. The bisphosphonate zoledronic acid impairs Ras membrane [correction of impairs membrane] localisation and induces cytochrome c release in breast cancer cells. Br J Cancer 2002;86:1479–86.
[14] Nishida S, Kikuichi S, Haga H, Yoshioka S, Tsubaki M, Fujii K, et al. Apoptosis-inducing effect of a new bisphosphonate, YM529, on various hematopoietic tumor cell lines. Biol Pharm Bull 2003;26:96–100.
[15] Benford HL, McGowan NW, Helfrich MH, Nuttall ME, Rogers MJ. Visualization of bisphosphonate-induced caspase-3 activity in apoptotic osteoclasts in vitro. Bone 2001;28:465–73.
[16] Coxon FP, Helfrich MH, Van't Hof R, Sebti S, Ralston SH, Hamilton A, et al. Protein geranylgeranylation is required for osteoclast formation, function, and survival: inhibition by bisphosphonates and GGTI-298. J Bone Miner Res 2000;15:1467–76.
[17] Monkkonen J, van Rooijen N, Ylitalo P. Effects of clodronate and pamidronate on splenic and hepatic phagocytic cells of mice. Pharmacol Toxicol 1991;68:284–6.
[18] Ailenberg M, Silverman M. Cytochalasin D disruption of actin filaments in 3T3 cells produces an anti-apoptotic response by activating gelatinase A extracellularly and initiating intracellular survival signals. Biochim Biophys Acta 2003;1593:249–58.
[19] Suria H, Chau LA, Negrou E, Kelvin DJ, Madrenas J. Cytoskeletal disruption induces T cell apoptosis by a caspase-3 mediated mechanism. Life Sci 1999;65:2697–707.
[20] Kim SJ, Hwang SG, Kim IC, Chun JS. Actin cytoskeletal architecture regulates nitric oxide-induced apoptosis, dedifferentiation, and cyclooxygenase-2 expression in articular chondrocytes via mitogen-activated protein kinase and protein kinase C pathways. J Biol Chem 2003;278:42448–56.
[21] Bando M, Miyake Y, Shiina M, Wachi M, Nagai K, Kataoka T. Actin cytoskeleton is required for early apoptosis signaling induced by anti-Fas antibody but not Fas ligand in murine B lymphoma A20 cells. Biochem Biophys Res Commun 2002;290:268–74.
[22] Melamed I, Gelfand EW. Microfilament assembly is involved in B-cell apoptosis. Cell Immunol 1999;194:136–42.
[23] Burton K. A study of the conditions and mechanisms of the diphenylamine reaction for the colorimetric estimation of deoxyribonucleic acid. Biochem J 1956;62:315–23.
[24] Arita K, Yamamoto Y, Takehara Y, Utsumi T, Kanno T, Miyaguchi C, et al. Mechanisms of enhanced apoptosis in HL-60 cells by UV-irradiated n-3 and n-6 polyunsaturated fatty acids. Free Radic Biol Med 2003;35:189–99.
[25] Yabuki M, Kariya S, Ishisaka R, Yasuda T, Yoshioka T, Horton AA, et al. Resistance to nitric oxide-mediated apoptosis in HL-60 variant cells is associated with increased activities of Cu, Zn-superoxide dismutase and catalase. Free Radic Biol Med 1999;26:325–32.
[26] Okada S, Yabuki M, Kanno T, Hamazaki K, Yoshioka T, Yasuda T, et al. Geranylgeranylacetone induces apoptosis in HL-60 cells. Cell Struct Funct 1999;24:161–8.
[27] Inoue A, Muranaka S, Fujita F, Kanno T, Tamai H, Utsumi K. Molecular mechanism of diclofenac-induced apoptosis of promyelocytic leukemia: dependency on ROS, Akt, Bid, Cyt. c and caspase pathway. Free Rad Biol Med 2004;37:1290–9.
[28] Bradford MM. A rapid and sensitive method for the quantitation of microgram quantities of protein utilizing the principle of protein-dye binding. Anal Biochem 1976;72:248–54.
[29] Salvioli S, Ardizzoni A, Franceschi C, Cossarizza A. JC-1, but not DiOC6(3) or rhodamine 123, is a reliable fluorescent probe to assess delta psi changes in intact cells: implications for studies on mitochondrial functionality during apoptosis. FEBS Lett 1997;411:77–82.
[30] Reed JC. Cytochrome c: can't live with it- can't live without it. Cell 1997;91:559–62.
[31] Luo X, Budihardjo I, Zou H, Slaughter C, Wang X. Bid, a Bcl-2 interacting protein, mediates cytochrome c release from mitochondria in response to activation of cell surface death receptors. Cell 1998;94:481–90.
[32] Li H, Zhu H, Xu CJ, Yuan J. Cleavage of BID by caspase 8 mediates the mitochondrial damage in the Fas pathway of apoptosis. Cell 1998;94:491–501.
[33] Kluck RM, Esposti MD, Perkins G, Renken C, Kuwana T, Bossy-Wetzel E, et al. The pro-apoptotic proteins, Bid, and Bax, cause a

limited permeabilization of the mitochondrial outer membrane that is enhanced by cytosol. J Cell Biol 1999;147:809–22.

[34] Yamada K, Arita K, Kobuchi H, Yamamoto S, Yoshioka T, Tamai H, et al. Cholesteryl-hemisuccinate-induced apoptosis of promyelocytic leukemia HL-60 cells through a cyclosporin A-insensitive mechanism. Biochem Pharmacol 2003;65:339–48.

[35] Gonzalez-Robayna IJ, Falender AE, Ochsner S, Firestone GL, Richards JS. Follicle-stimulating hormone (FSH) stimulates phosphorylation and activation of protein kinase B (PKB/Akt) and serum and glucocorticoid-induced kinase (Sgk): evidence for A kinase-independent signaling by FSH in granulose cells. Mol Endocrinol 2000;14:1283–300.

[36] Tsygankova OM, Saavedra A, Rebhun JF, Quilliam LA, Meinkoth JL. Coordinated regulation of Rap1 and thyroid differentiation by cyclic AMP and protein kinase A. Mol Cell Biol 2001;21:1921–9.

[37] Gross A, McDonnell JM, Korsmeyer SJ. BCL-2 family members and the mitochondria in apoptosis. Genes Dev 1999;13:1899–911.

[38] Breitschopf K, Haendeler J, Malchow P, Zeiher AM, Dimmeler S. Posttranslational modification of Bcl-2 facilitates its proteasome-dependent degradation: molecular characterization of the involved signaling pathway. Mol Cell Biol 2000;20:1886–96.

[39] Shack S, Gorospe M, Fawcett TW, Hudgins WR, Holbrook NJ. Activation of the cholesterol pathway and Ras maturation in response to stress. Oncogene 1999;18:6021–8.

[40] Okada S, Yabuki M, Kanno T, Hamazaki K, Yoshioka T, Yasuda T, et al. Geranylgeranylacetone induces apoptosis in HL-60 cells. Cell Struct Funct 1999;24:161–8.

[41] Senaratne SG, Mansi JL, Colston KW. The bisphosphonate zoledronic acid impairs Ras membrane [correction of impairs membrane] localisation and induces cytochrome c release in breast cancer cells. Br J Cancer 2002;86:1479–86.

[42] Erhardt P, Schremser EJ, Cooper GM. B-Raf inhibits programmed cell death downstream of cytochrome c release from mitochondria by activating the MEK/Erk pathway. Mol Cell Biol 1999;19: 5308–15.

[43] Chang F, Steelman LS, Shelton JG, Lee JT, Navolanic PM, Blalock WL, et al. Regulation of cell cycle progression and apoptosis by the Ras/Raf/MEK/ERK pathway (ew). Int J Oncol 2003;22:469–80.

[44] Bonni A, Brunet A, West AE, Datta SR, Takasu MA, Greenberg ME. Cell survival promoted by the Ras-MAPK signaling pathway by transcription-dependent and -independent mechanisms. Science 1999;286:1358–62.

[45] Fang X, Yu S, Eder A, Mao M, Bast Jr RC, Boyd D, et al. Regulation of BAD phosphorylation at serine 112 by the Ras-mitogen-activated protein kinase pathway. Oncogene 1999;18:6635–40.

[46] Lam M, Oleinick NL, Nieminen AL. Photodynamic therapy-induced apoptosis in epidermoid carcinoma cells. Reactive oxygen species and mitochondrial inner membrane permeabilization. J Biol Chem 2001;276:47379–86.

[47] Slee EA, Harte MT, Kluck RM, Wolf BB, Casiano CA, Newmeyer DD, et al. Ordering the cytochrome c-initiated caspase cascade: hierarchical activation of caspases-2, -3, -6, -7, -8, and -10 in a caspase-9-dependent manner. J Cell Biol 1999;144:281–92.

[48] Axline SG, Reaven EP. Inhibition of phagocytosis and plasma membrane mobility of the cultivated macrophage by cytochalasin B. Role of subplasmalemmal microfilaments. J Cell Biol 1974;62:647–59.

[49] Jackman MR, Shurety W, Ellis JA, Luzio JP. Inhibition of apical but not basolateral endocytosis of ricin and folate in Caco-2 cells by cytochalasin D. J Cell Sci 1994;107:2547–56.

[50] Gottlieb TA, Ivanov IE, Adesnik M, Sabatini DD. Actin microfilaments play a critical role in endocytosis at the apical but not the basolateral surface of polarized epithelial cells. J Cell Biol 1993;120:695–710.

[51] Frith JC, Rogers MJ. Antagonistic effects of different classes of bisphosphonates in osteoclasts and macrophages in vitro. J Bone Miner Res 2003;18:204–12.

[52] Rogers MJ, Xiong X, Ji X, Monkkonen J, Russell RG, Williamson MP, et al. Inhibition of growth of Dictyostelium discoideum amoebae by bisphosphonate drugs is dependent on cellular uptake. Pharm Res 1997;14:625–30.